Electroosmotic Flow Can Generate Ion Current Rectification in Nano- and Micropores

Erik C. Yusko,[†] Ran An,[†,‡] and Michael Mayer[†,*]

[†]Department of Biomedical Engineering, and [‡]Center for Ultrafast Optical Science, University of Michigan, Ann Arbor, Michigan, 48109-2110

ABSTRACT This paper introduces a strategy for generating ion current rectification through nano- and micropores. This method generates ion current rectification by electroosmotic-driven flow of liquids of varying viscosity (and hence varying conductance) into or out of the narrowest constriction of a pore. The magnitude of current rectification was described by a rectification factor, R_f, which is defined by the ratio of the current measured at a positive voltage divided by the current measured at a negative voltage. This method achieved rectification factors in the range of 5—15 using pores with diameters ranging from 10 nm to 2.2 μm. These R_f values are similar to the rectification factors reported in other nanopore-based methods that did not employ segmented surface charges. Interestingly, this work showed that in cylindrical nanopores with diameters of 10 nm and a length of at least 275 nm, electroosmotic flow was present and could generate ion current rectification. Unlike previous methods for generating ion current rectification that require nanopores with diameters comparable to the Debye length, this work demonstrated ion current rectification in micropores with diameters 500 times larger than the Debye length. Thus this method extends the concept of fluidic diodes to the micropore range. Several experiments designed to alter or remove electroosmotic flow through the pore demonstrated that electroosmotic flow was required for the mode of ion current rectification reported here. Consequently, the magnitude of current rectification could be used to indicate the presence of electroosmotic flow and the breakdown of electroosmotic flow with decreasing ionic strength and hence increasing electric double layer overlap inside nanopores.

KEYWORDS: nanopore · micropore · electroosmotic flow · Debye length · electric double layer · current rectification · fluidic diode

This paper describes a method for generating ion current rectification by employing electroosmotic flow to fill the narrowest constriction of a pore with either a solution of low or high ionic conductance. This approach extends the phenomenon of ion current rectification from solid-state nanopores to micropores. Solid-state nanopores and nanochannels are attracting increasing attention in areas of fluidic logic circuits, also called iontronics, due to their ability to rectify ion current.[1,2] Recent advances in nanotechnology have permitted the fabrication of pores with diameters as small as 1 nm.[3−8] Such small pores open the door for fundamental studies of electrostatic interactions or steric hindrance that ions may experience in nanoscale transport.[9,10] The first examples of non-ohmic ion transport in pores filled with aqueous solutions without implementing mechanical components were demonstrated in conical glass pipettes by Wei, Bard, and Feldberg in 1997.[11] More recently, Siwy's group demonstrated that an electric potential difference across nanopores can result in controlled mass transport, selective ion flow, and ion current rectification.[10,12−14] Ion current rectification in nanopores is of interest because many ion-channel proteins in cellular membranes are rectifying and because ion current rectification is analogous to electronic diodes.[15] These electronic diodes are important circuit elements because they can rectify electron current in response to an electric potential difference. Fluidic diodes, in contrast, rectify ionic current in a liquid. Thus, ion current rectification in nanopores can be used to control ion concentrations in nano- and microfluidic systems.[16,17] Other applications entail the use of nanopore-based current rectifiers for biosensors or for logic gates and diodes in fluidic circuits.[1,10,18−20]

The extent of ion flux in one direction through a pore relative to the ion flux in the other direction determines the quality of a fluidic diode. The magnitude of ion current rectification is typically quantified by the rectification factor, R_f. The rectification factor is measured at a specific potential difference, and it is defined as the ratio between the average currents at opposite polarities (*i.e.*, $R_f = I_+/I_-$ in which I_+ is the current at a positive potential difference and I_- is the current at the same but negative potential difference).[11] Techniques to increase R_f include the fabrication of pores with very small diameters (1−20 nm), selection of an optimum ionic strength of the

*Address correspondence to mimayer@umich.edu.

Received for review October 1, 2009 and accepted December 07, 2009.

Published online December 22, 2009.
10.1021/nn9013438

electrolyte solution, and methods to generate or segment charges on the channel walls inside of nanopores.[21]

Here, we present a method that uses pores to connect two separate solutions of different conductance in order to generate ion current rectification in nanopores (10−30 nm) and in micropores (0.5−2.2 μm). These micropores had diameters ~500 times larger than Debye length and ~ 50 times larger than the largest pores currently capable to act as ion current rectifiers.[11,22]

Ion current rectification in nanopores is a consequence of electrostatic interactions between the substrate of the pore and the electrolyte solution.[10,11,13,23] Due to the surface charge of the substrate, ions of the same charge polarity as the substrate material (referred to as co-ions) are depleted from the solution near the substrate, whereas ions with an opposite charge than the pore substrate (referred to as counter-ions) accumulate in solution near the substrate. The region near the surface in which co-ions are excluded and counter-ions are accumulated is referred to as the electric double layer.[24] The thickness of the electric double layer is characterized by the Debye screening length. In aqueous solutions of a monovalent salt, eq 1 describes the Debye screening length, κ^{-1} (m):

$$\kappa^{-1} = \sqrt{\frac{\varepsilon_r \varepsilon_o RT}{2F^2 C_o}} \quad (1)$$

where ε_r (unitless) is the dielectric constant of the solvent, ε_o ($C^2 \cdot N^{-1} \cdot m^{-2}$) is the permittivity of vacuum, R ($J \cdot K^{-1} \cdot mol^{-1}$) is the universal gas constant, T (K) is the absolute temperature, F ($C \cdot mol^{-1}$) is the Faraday constant, and C_o ($mol \cdot m^{-3}$) is the bulk concentration of the salt.[25] In addition to the ionic strength and the dielectric constant of the solvent, the surface charge density of the substrate affects the electric double layer. The Poisson−Nernst−Planck equations can be used to account for the surface charge densities in modeling ion transport through pores.[26] In aqueous solutions that contain a monovalent salt, the Debye length ranges from less than 1 nm at a concentration of 1.0 M to ~ 10 nm at a concentration of 1 mM. In nanopores with diameters on the order of the Debye length, the electric double layer can occupy a significant cross-section of the pore and may even overlap within the pore.[27] This condition, referred to as electric double layer overlap, results in exclusion of co-ions from the pore and accumulation of counterions within the pore. This preferential accumulation and depletion of ions as a consequence of a Debye length comparable to the diameter of the pore is one requirement for traditional fluidic diodes that are based on nanopores.[22,28]

The second requirement for ion current rectification in nanopores is an asymmetry in the distribution of ions along the length axis of the nanopore.[28] Under symmetric conditions (*i.e.*, a cylindrical pore between two identical solutions), a Debye length on the order of the nanopore does not result in ion current rectification. In contrast, under asymmetric conditions (*i.e.*, a conical pore,[11−13,22,29−35] a pore between solutions with different ionic strength, a pore between solutions with different pH,[37] or a pore with segmented surface charges,[4,12,13,23,38]) an asymmetric distribution of ions is formed along the length axis of pores.[39,40] Consequently, the nanopore exhibits reduced or enhanced permeability of the conducting ions through the pore depending on the direction of the electric field. For instance, a conical nanopore with a negative surface charge shows increased conductance if the narrow opening of the pore faces the anode and the net flow of cations through the pore is directed from the narrow tip toward the large base of the conical pore. Conversely, the conductance through the same pore is reduced at the opposite polarity in which the net flow of cations through the conical nanopore is directed from the large base toward the narrow tip.[29,41] Wei *et al.* first demonstrated ion current rectification in conical nanopipettes with the narrowest diameter ~20 times larger than the Debye length.[11] Since then, Siwy's group, Ensinger's group, and others observed ion current rectification in conical nanopores with the narrowest diameter up to ~60 times larger than Debye length.[12,13,21,22,32−35,42,43] These studies obtained R_f values of 6−20. An asymmetric double layer generated in nanopores that separated solutions with different ionic strength or pH resulted in similar values for R_f.[22,36] Finally, an asymmetric double layer that was generated by different charges exposed at different regions on the surface within a pore (*i.e.*, a positive charge density at one end of the pore and a negative charge density at the other end) resulted in R_f values of 100−321.[4,12,23] Heins *et al.* also generated asymmetry by the addition of 1,4,7,10,13,16-hexaoxacyclooctadecane to one solution compartment. This molecule formed a complex with potassium ions, and caused an increase in R_f from ~2.5 to ~19 in nanopores with diameters less than 3 nm.[10] In summary, existing methods for inducing ion current rectification within nanpores must fulfill two requirements: (1) at least one dimension of the channel or pore must be on the order of the Debye length, and (2) charge asymmetry within the pore must be induced.[28]

Here, we present a method for generating ion current rectification in pores with diameters considerably larger than the Debye length. To explain how this method results in current rectification we emphasize that in an electric field the electric double layer affects two types of ion transport: electrophoretic migration and electroosmotic flow (EOF). Electrophoretic migration describes the movement of ions in response to an electric field, while EOF describes the plug flow of a so-

lution induced by the movement of the electric double layer in an electric field.[44] The major distinction between these two types of transport is that cations and anions move in different directions in electrophoretic migration, whereas EOF results in bulk fluid movement toward the fluid compartment that is biased with the same polarity as the charge on the substrate of the pore wall. For instance, in the case of materials with a negative surface charge, the direction of the EOF is always toward the cathode. Since EOF is induced by the movement of the electric double layer, it collapses in pores in which the electric double layers overlap significantly.[45−48] In this case, electrophoretic migration is the dominant mechanism of ion transport.[47] Thus, in nanopores that exhibit ion current rectification—and hence require the pore diameter to be comparable to the Debye length—EOF is typically not considered to be a major contributor to ion current rectification.[31,49−51] Daiguji *et al.* estimated that EOF contributes less than 10% to ion transport in nanofluidic channels with channel heights of 30 nm and a surface charge density ranging from −0.1 to −1.0 $mC \cdot m^{-2}$ in solutions containing 0.1 mM of a monovalent salt.[50] White *et al.* recently modeled the contribution of EOF to ion transport under conditions of electric double layer overlap and found that EOF started to contribute to a small but noticeable extent when the electric potential difference exceeded 0.3 V.[31] Unlike these previous studies, we present a method for generating ion current rectification that favors and takes advantage of EOF.

Using this EOF-based method, we first demonstrate that EOF-driven flow of liquids of varying viscosity (and hence conductance) into or out of the narrowest constriction of a pore can generate ion current rectification in nano- and micropores. Thus, this method introduces the concept of an electroosmotic diode. These electroosmotic diodes achieved similar rectification factors to nanopores without segmented surface charges, with R_f values ranging from 5 to 15. Unlike previous studies, these electroosmotic diodes can generate ion current rectification in pores with diameters that are 500 times larger than the Debye length and thus extend the phenomenon of ion current rectification from nanopores to micropores.

For comparison, we also investigated the concept of electroosmotic diodes in cylindrical nanopores with diameters on the order of the Debye length. We confirmed that electroosmotic diodes continue to rectify current in nanopores until the Debye length was equal to the diameter of the pore. We also show that incomplete electric double layer overlap in a pore with a diameter on the order of the Debye length resulted in rectification factors *greater* than the rectification factor we would expect for electroosmotic diodes—an effect that we attribute to the synergistic combination of the characteristics of a traditional rectifying nanopore and the

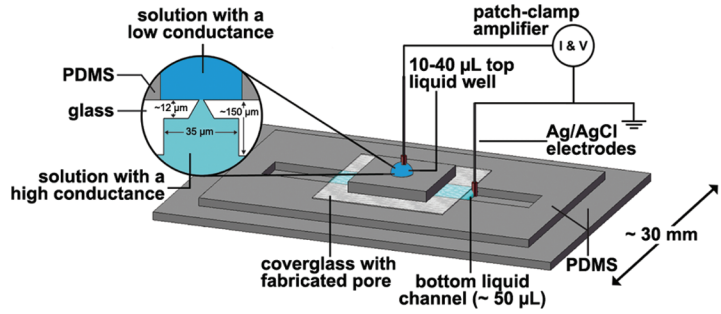

Figure 1. Schematic diagram of the experimental setup for recording ion currents through nano- and micropores. The inset depicts a cross-sectional view of a conical pore fabricated in a borosilicate cover glass. This figure does not show the cylindrical pore with a diameter of 10 nm in a PET film or the cylindrical pores with diameters of 30 nm in silicon nitride, but these pores were mounted in a similar fashion in the device. For all experiments, unless noted otherwise, the low-conductance solution filled the top compartment and the high-conductance solution filled the bottom compartment. For all experiments and current−voltage curves, the polarity of the voltage was defined by the electrode in the top liquid compartment, while the electrode in the bottom compartment was connected to ground.

electroosmotic diode. Quantitative analysis of the ion current rectification of such hybrid pores provided a simple way of testing the significance of EOF with regard to current rectification as a function of the Debye length. This paper hence introduces a novel type of fluidic diode, provides experimental evidence for the presence and breakdown of EOF in nanopores, and quantifies the degree of double layer overlap necessary for this breakdown.

RESULTS AND DISCUSSION

Electroosmotic Flow of Solutions of Different Conductance Can Generate Ion Current Rectification in Nano- and Micropores. To explore ion current rectification in a system that connects two solutions of different conductance with a nano- or micropore, we measured the ionic current through a conical pore with a tip diameter of 500 nm in a glass slide. For this experiment, we prepared two solutions of equal electrolyte concentration (*i.e.*, 5 mM KCl) but of different solvent composition and hence different conductance. The conductance of one solution was 933 $\mu S \cdot cm^{-1}$ (prepared in pure water with a KCl concentration of 5 mM), and the conductance of the second solution was 185 $\mu S \cdot cm^{-1}$ (prepared in 75% (v/v) DMSO and 25% (v/v) water with a final KCl concentration of 5 mM in the mixture). The different conductance for these solutions is a consequence of their different viscosity; according to the Nernst−Einstein relation, the mobility of small ions is inversely proportional to the viscosity of the solvent.[52]

Figure 1 illustrates the recording setup and the location of the two different solutions during experiments. Figure 2A shows current *versus* voltage plots, whose slopes reflect the conductance when the same solution occupied both fluid compartments of the setup. As expected, the behavior of such a system was ohmic, that is, the current was directly proportional to the potential difference over the entire range. Figure 2A also

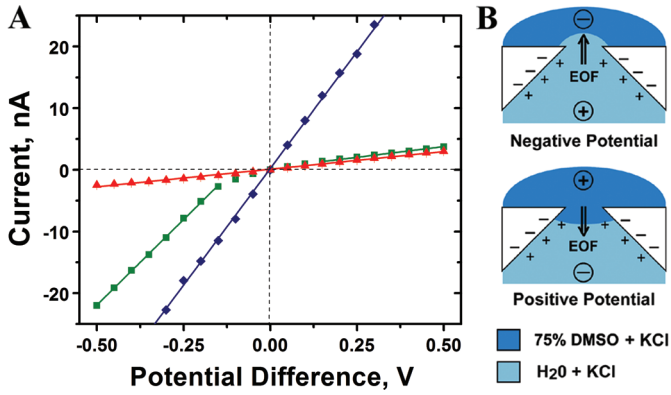

Figure 2. Current−voltage curves measured using a conical, submicrometer pore in glass with a tip diameter of 500 nm and illustration of the concept of an electroosmotic diode. (A) Ion current rectification due to positioning of two different solutions with high or low conductance in the narrowest part of the pore. Curves were fit with a linear best fit of the form $I = R^{-1}V + B$. Where I is the current (A), V is the applied electric potential (V), B (A) is the y-intercept of the line, and R is the resistance (Ω). In the experiment in which the pore separated two different solutions, the currents recorded in the nonlinear range from −150 to +150 mV were omitted from the best-fit analysis (see main text for an explanation). Resistance values from the linear fits were as follows: KCl in pure H_2O in both compartments (◆) R = 13.2 MΩ; KCl in 75% (v/v) DMSO and 25% (v/v) H_2O in both compartments (▲) R = 175.0 MΩ; and when the pore separated the two different solutions (■) R = 144.0 MΩ at positive voltages and R = 18.0 MΩ at negative voltages. All solutions contained a final concentration of 5 mM KCl. (B) Suggested principle of operation of an electroosmotic diode. For the negatively charged glass surface, the EOF is always directed toward the cathode; thus, under a positive potential, the EOF moved the solution from the anode compartment located on top of the chip (low-conductance solution) into the narrowest constriction of the pore, while at a negative potential, the EOF moved the solution from the anode compartment located below the chip (high-conductance solution) into the narrowest constriction of the pore.

shows a current−voltage plot when the conical pore separated two different solutions. Under these conditions, the pore rectified ion currents: at positive potentials (the polarity of the potential difference refers to the electrode located in the top fluid compartment of the setup shown in Figure 1), the magnitude of the current was significantly smaller than at negative potentials. Figure 3A shows a current−voltage curve using the same solutions but with a large, conical micropore (tip diameter of 2.2 μm). Remarkably, we observed similar ion current rectification in both pores, although their diameters were well above the Debye length (κ^{-1} in the low conductance solution was ~3.3 nm and in the high conductance solution it was ~4.3, see Table 1). As a control experiment, we switched the location of the solutions in the experimental setup such that the solution with low conductance (185 $\mu S \cdot cm^{-1}$) filled the bottom compartment and the solution with high conductance (933 $\mu S \cdot cm^{-1}$) filled the top compartment. Figure 3B shows that under these conditions, we observed ion current rectification at the expected reversed polarity, that is, decreased current at negative potentials rather than at positive potentials. Interestingly, the slope at negative potentials in Figure 3B was smaller than the slope at positive potentials in Figure 2. We attribute the reduced slope in Figure 3B to an increased

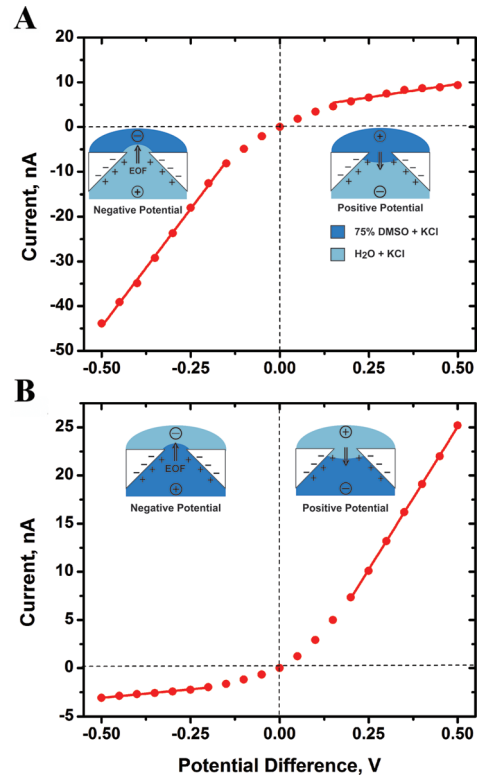

Figure 3. Ion current rectification employing the concept of an electroosmotic diode in micropores and a control experiment, in which the location of the two solutions relative to the conical pore and electrodes was reversed. (A) Ion current rectification in a conical micropore with a tip diameter of 2.2 μm and all other dimensions as depicted in Figure 1. The R_f value in this pore was 5. The solution in the top compartment contained 5 mM KCl in 75% (v/v) DMSO and 25% (v/v) water (low conductance), whereas the solution in the bottom compartment contained 5 mM KCl in deionized water (high conductance). (B) Current *versus* voltage curve in a conical pore with a tip diameter of 500 nm. In this control experiment, the location of both solutions was reversed, that is, the solution in the bottom compartment had a low conductance and contained 5 mM KCl in 75% (v/v) DMSO and 25% (v/v) water, whereas the solution in the top compartment had a high conductance and contained 5 mM KCl in pure water. In agreement with the direction of EOF, the direction of ion current rectification was reversed from that with the original location of the solutions as shown in Figure 2. The insets describe the direction of the EOF and the proposed position of the two solutions within the pore at a positive and negative polarity applied to the top compartment. The R_f value in this configuration was ~7.

TABLE 1. Debye Lengths for Various Concentrations of KCl in Pure Water and Pure DMSO

[KCl] (mM)	κ^{-1} in water[a] (nm)	κ^{-1} in DMSO[a] (nm)
1	9.58	7.43
5	4.26	3.32
15	2.49	1.92
50	1.36	1.05
100	0.96	0.74
150	0.78	0.61
175	0.73	0.56
200	0.68	0.52

[a]Debye lengths were calculated for a system at 25 °C. Relative dielectric constants, ε_r, of 78.36 and 46.5 were used for water and DMSO, respectively. [53,54]

resistance through the entire conical pore and access channel for the configuration in Figure 3B, in which the solution with low conductance occupied the entire access channel and conical pore. Conversely, in Figure 2 the solution with low conductance likely only occupied the narrowest constriction of the conical pore while mixing more and more with the solution of high conductance along the length of the pore.

For the configuration that placed the low-conductance solution in the top compartment, we hypothesized that, at positive voltages, the low current was due to the EOF-driven flow of the low-conductance solution from the anode compartment into the pore. Similarly, at negative voltages, the high current was due to EOF-driven flow in the opposite direction, which moved the solution with a high conductance into the pore. To test this hypothesis we compared the $I-V$ characteristics of the pore when it connected a solution of low conductance and a solution of high conductance to the $I-V$ characteristics of the same pore when it connected two identical solutions, which were both either of low or high conductance. Since the resistance between the Ag/AgCl electrodes is dominated by the narrowest constriction of the pore, we expected that the resistance through the pore at a given polarity would indicate whether the low-conductance solution or the high-conductance solution filled the pore. Thus, we hypothesized that if the low-conductance solution filled the pore then the resistance would be comparable to a situation when only the low-conductance solution was used. Similarly, if the high-conductance solution filled the pore then the resistance would be comparable to a situation when only the high-conductance solution was used. We measured the resistance from the linear regions of the current *versus* voltage plots in Figure 2A. As expected, under conditions where the pore separated two different solutions, the resistance of 18.0 MΩ at a negative potential was similar (within ±30%) to the resistance of 13.2 MΩ that we observed when the pore separated two identical, high-conductance solutions. In a similar fashion, when the pore separated the two different solutions, the resistance of 144.0 MΩ at a positive potential, was similar (within ±30%) to the resistance of 175 MΩ that we observed when the pore separated two identical, low-conductance solutions. These results support the hypothesis that when two different solutions were separated by a pore, either the solution with low conductance (185 $\mu S \cdot cm^{-1}$) or the solution with high conductance (933 $\mu S \cdot cm^{-1}$) dominated the overall resistance through the pore. Thus, we propose that EOF moved the solution with low conductance into the narrowest constriction of the pore under positive potentials, whereas it moved the solution with high conductance into the pore under negative potentials. Figure 2B illustrates this proposed mechanism.

On the basis of this mechanism of operation, we propose that the nonlinear regions of the current−voltage curves in Figure 2A and 3 are the result of mixing of the two different solutions within the narrowest part of the pore. In contrast, we attribute the linear regions of the current−voltage plot at potentials above |±150| mV to EOF-driven flow of the almost unmixed solutions from either the top fluid compartment or the bottom fluid compartment into the narrowest constriction of the pore. We hypothesize that in the absence of an electric field, the solutions on either side of the pore mixed diffusively in the fluid filled pore, and we propose that in the presence of an electric field, the EOF added a convective component of fluid and ion transport within the pore. In the absence of electric double layer overlap, the magnitude of EOF, expressed as electroosmotic mobility, u_{eo} ($m \cdot s^{-1}$), is dependent on the electric field strength, E ($V \cdot m^{-1}$), the zeta potential, ζ (V), and the viscosity, η ($Pa \cdot s$), of the electrolyte:[25]

$$u_{eo} = \frac{\varepsilon_r \varepsilon_o \zeta E}{\eta} \quad (2)$$

The zeta potential ζ is given by

$$\zeta \cong \frac{\kappa^{-1}\sigma}{\varepsilon_r \varepsilon_o} \quad (3)$$

with σ ($C \cdot m^{-2}$) corresponding to the excess surface charge on the pore wall.[25] As the EOF increases with increasing electric field, we suggest that at a critical potential difference (here ≥ |± 150| mV), the EOF was sufficiently large to overcome most of the diffusive mixing and to fill the narrowest part of the pore with the solution from the anode compartment (*i.e.*, the low-conductance solution or the high-conductance solution depending on the polarity). As a consequence of this mechanism, we hypothesized that in the range of −150 to +150 mV, the relatively small electric field generated a slow EOF that allowed mixing of the solutions to occur in the pore. This mixing would result in an intermediate conductance of the solution within the pore and hence explain the intermediate current we observed in the region of −150 to + 150 mV. Figure 2 panels B and C illustrate the location of the two solutions within the pore at a potential difference greater than |± 150| mV.

The Ratio between the Conductance of Both Solutions Agreed with the Rectification Factors. To provide further evidence that EOF was responsible for the rectification of ion current by driving a solution of high or low conductance from the anode compartment into the narrowest constriction of the pore, we compared the ratio between the conductance of both solutions determined with a conductance meter to the rectification factors that we obtained when using the respective pair of these two solutions in the top and bottom fluid compartments of

TABLE 2. Conductance of Solutions Used in Experiments

[KCl] (mM)	solvent	conductance[a] ($\mu S \cdot cm^{-1}$)	G_f[b]	R_f[a,c]	Δ %
5.0	Pure H_2O	2,115 ± 19	1.0		
50.0	Pure H_2O	8,480 ± 46	1.0		
100.0	Pure H_2O	15,993 ± 90	1.0		
5.0	75% DMSO + 25% H_2O	401 ± 8	5.3 ± 0.1	5.3 ± 0.8	0
50.0	75% DMSO + 25% H_2O	1,476 ± 14	5.7 ± 0.1	5.1 ± 1.2	−11
100.0	75% DMSO + 25% H_2O	2,595 ± 25	6.2 ± 0.1	4.6 ± 0.9	−26
50.0	75% isopropanol + 25% H_2O	978 ± 19	8.6 ± 0.3	6.4 ± 2.1	−26
50.0	66% glycerol + 25% H_2O	579 ± 11	14.6 ± 0.2	12.9 ± 1.0	−12

[a]Standard deviations were obtained from at least three observations. All measurements were taken at a room temperature of 21 ± 2 °C. [b]The conductance factor, G_f, was calculated with eq 5. [c]R_f was determined from experiments in which a conical pore in glass with a tip diameter of 500 nm separated the solvent and water mixture (low-conductance solution, located in the top fluid compartment) from a solution with an identical concentration of KCl in pure water (high-conductance solution, located in the bottom fluid compartment).

the setup shown in Figure 1. Again, we used a conical nanopore with a tip diameter of 500 nm that was significantly larger than the Debye length and hence, excluded the possibility of electric double layer overlap (Table 1). The electrical resistance of a conical nanopore, R_p (Ω), is inversely proportional to the conductance of the solution, G ($\Omega^{-1} \cdot m^{-1}$), in the pore and can be estimated with[14]

$$R_p = \frac{4L}{G\pi Dd} \quad (4)$$

where L (m) is the length of the pore, D (m) is the diameter of the large opening, d (m) is the diameter of the small opening, and G is the conductance of the solution within the pore. On the basis of the relationship between the resistance of the pore and the conductance of the solution residing in the pore, we expected the ratio of the conductance values for a solution with high conductance to that of a solution with low conductance to be equal to the rectification factor that occurred when the pore was filled by EOF with either one of those solutions. We define a conductance factor, G_f, as the ratio between a solution with high conductance, G_{H_2O}, to a solution with low conductance, G_{mix}:

$$G_f = \frac{G_{H_2O}}{G_{mix}} \quad (5)$$

Table 2 summarizes the conductance values of all solutions, the G_f values for the specified mixture relative to the same ion concentration prepared in pure water, and the corresponding R_f values for the specified mixture in the top compartment and the aqueous solution in the bottom compartment. We measured values for R_f from the current we observed at a potential difference of +0.5 and −0.5 V. The general agreement (within ±30%) between the values of G_f and R_f suggests that at a potential difference above |± 150| mV the narrowest diameter of the pore (the part with the largest resistance) was filled predominantly with the solution from the anode compartment. Depending on the polarity of the potential difference, this solution was either the top solution or the bottom solution and hence either the solution with a high or low conductance.

To confirm that ion current rectification was independent of the electrolyte concentration, we compared the G_f and R_f values at KCl concentrations of 5.0, 50.0, and 100.0 mM in experiments in which the pore separated the KCl solution prepared in 75% (v/v) DMSO and 25% (v/v) water (top compartment) from a KCl solution prepared in pure water (bottom compartment). Table 2 summarizes the resulting R_f and G_f values. We found a similar R_f value for all concentrations of KCl and good agreement (within ±26%) between the R_f and the G_f values.

To explore the possibility of controlling the rectification factors with this system, we prepared three solvent mixtures with different volume fractions of water with organic solvent (DMSO, isopropyl alcohol, or glycerol) and hence different viscosity. Table 2 summarizes the conductance values of these solutions. For each of the mixtures, we observed a unique R_f when the pore separated a mixed, low-conductance solution containing the specified concentration of KCl from a high-conductance solution prepared in pure water but with the same concentration of KCl. Again, the G_f and R_f values agreed within ±26%. The combination of 50 mM KCl in pure water (in the bottom compartment) with a solution of 50 mM KCl prepared in 66% (v/v) glycerol and 34% (v/v) H_2O (in the top compartment) resulted in the largest rectification factor with an average value of R_f = 12.9, followed by a solution of 75% (v/v) isopropyl alcohol and 25% H_2O (v/v) in the top compartment with R_f = 6.4 and a solution of 75% (v/v) DMSO and 25% H_2O (v/v) in the top compartment with R_f = 5.1. The general agreement between the G_f and R_f values provides further evidence that the resistance of the pore in this two-solution system was dependent on the solution that occupied the narrowest constriction of the pore and that the applied potential difference was able to drive the solution from either the top or the bottom fluid compartment into the pore.

Disruption of EOF Reduced Ion Current Rectification. To provide further evidence that EOF generated the ion current rectification reported here, we neutralized the negatively charged glass substrate of the pore to disrupt EOF. Electroosmotic flow is a consequence of the electrophoretic movement of the electric double layer in an applied electric field.[44] In negatively charged glass pores, cations comprise the electric double layer, and thus the EOF is directed toward the cathode. At strongly acidic pH (*e.g.*, pH = 0), the negatively charged silanol groups of the glass surface are neutralized by protonation. Hence the accumulation of cations near the surface is strongly reduced, and EOF is either absent or very slow.[22,29,55,56] Figure 4A shows that in agreement with neutralizing negative charges on the glass and hence preventing EOF at pH = 0, we did not observe significant ion current rectification (*i.e.*, $R_f \leq 1.4$) when the top compartment was filled with 1 M HCl in 75% (v/v) DMSO and 25% (v/v) H_2O (conductance = 20.34 $mS \cdot cm^{-1}$) and the bottom compartment was filled with 1 M HCl in pure water (conductance > 3000 $mS \cdot cm^{-1}$).

To provide additional evidence that EOF moved the solution from the anode compartment into the pore, we modified the glass substrate with a polycation (poly-L-lysine) to expose positive surface charges.[56] With positive surface charges immobilized on the wall of the pore, we hypothesized that anions would accumulate within the electric double layer, which would result in an EOF directed toward the anode rather than the cathode. The inset of Figure 4B illustrates the predicted surface charge, the direction of EOF, and the positions of both solutions under conditions of positive and negative potentials in the case of a pore with immobilized positive surface charges. The results in Figure 4B support this hypothesis: the absolute value of the current at a positive polarity was greater than the absolute value of the current at a negative polarity, and the direction of ion current rectification was reversed as expected for a reversed direction of EOF. We observed a rectification factor of $R_f = 4$ in this configuration. Together these results indicate that the effect of EOF determined which solution was dominant in the narrowest constriction of the pore and consequently generated ion current rectification.

EOF and Ion Current Rectification Break Down in Pores with Diameters Near the Size of the Debye Length. To examine EOF-induced ion current rectification as a function of the Debye length, in particular when the Debye length approached the diameter of the pore, we used a cylindrical nanopore with a diameter of 10 nm that was fabricated in a PET film with a thickness of 12 μm. To achieve varying Debye lengths, we prepared solutions with various concentrations of KCl in 75% (v/v) DMSO and 25% (v/v) water. We also prepared solutions with various concentrations of KCl in pure water. Table 1 summarizes the concentrations of KCl that we used

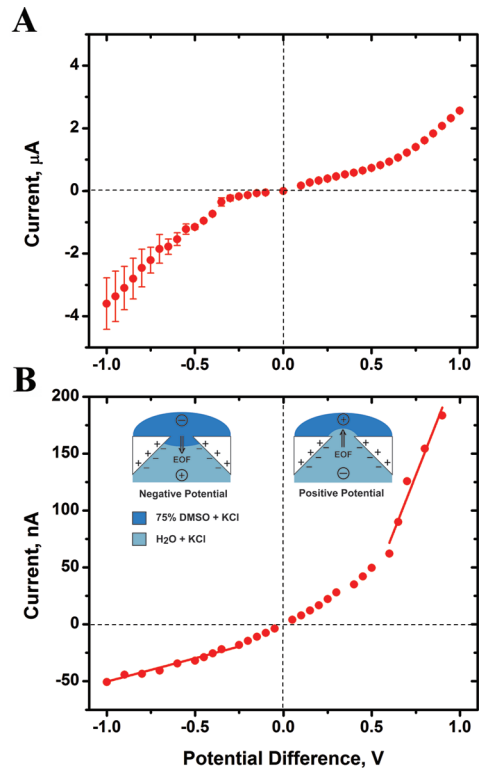

Figure 4. Effect of acidic pH or of physisorbed polycations on the current−voltage curve from a conical nanopore in glass with a tip diameter of 500 nm. (A) Current−voltage curve using solutions with a pH ≈ 0. Note the significantly reduced ion current rectification, $R_f = 1.4$. In this experiment, the bottom solution consisted of 1.0 M HCl in pure water with a conductance greater than 3000 $mS \cdot cm^{-1}$ and the top solution consisted of 1.0 M HCl in 75% (v/v) DMSO and 25% (v/v) H_2O with a conductance of 20.34 $mS \cdot cm^{-1}$. B) Pores with a positive surface charge (generated by physisorption of poly-L-lysine onto the glass substrate) resulted in a reversed direction of ion current rectification (*i.e.*, ion currents were reduced at the opposite polarity of that shown in Figure 2). (B inset) Illustration of the orientation of the pore, the two solutions, and the direction of EOF in a pore with positive charges immobilized on its surface. The solutions used to generate the *I*−*V* curve in panel B contained 50 mM KCl and 15 mM HEPES (pH = 7.5) prepared in pure water (bottom solution) and prepared in 75% (v/v) DMSO and 25% (v/v) H_2O (top solution).

for these experiments and the predicted Debye length for the various concentrations of KCl in pure water and in pure DMSO. The Debye length is smaller in pure DMSO than in water because the dielectric constant of DMSO is smaller than the dielectric constant of pure water. Figure 5A shows current−voltage curves for three KCl concentrations, which led to Debye lengths close to the diameter of the pore. At 1 mM KCl, the Debye length in pure water is 9.6 nm and hence close to the diameter of the pore. In this case we observed almost no ion current rectification and R_f was 1.1.

To investigate the effect of the Debye length on R_f systematically, we plotted R_f as a function of the nondimensional Debye length, $\lambda_D = \kappa^{-1}/d$, with d = 10 nm representing the diameter of the cylindrical nanopore (Figure 5B). Figure 5B also shows the nondimensional average-area velocity of electroosmotic flow predicted

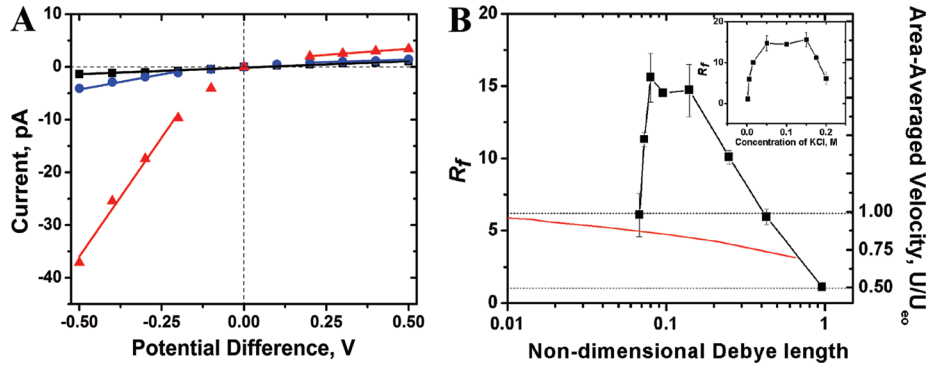

Figure 5. Current−voltage curves from a nanopore when the Debye length approached the diameter of the pore and rectification factors, R_f, as a function of the nondimensional Debye length. (A) Current−voltage curves for concentrations of KCl that generate a Debye length close to the diameter of the pore: Solutions were prepared in pure water (located in the bottom compartment), and in 75% (v/v) DMSO and 25% (v/v) water (located in the top compartment). Solutions contained (■) 1 mM KCl, (●) 1 5 mM KCl, and (▲) 50 mM KCl. (B) Rectification factors, R_f, as a function of the nondimensional Debye length (■), and the nondimensional area-averaged velocity of EOF (red line) as predicted by Taylor and Ren.[48] The nondimensional Debye length was calculated for KCl solutions in pure water. The inset in panel B depicts the rectification factor as a function of the concentration of KCl.

by Taylor and Ren as a function of the nondimensional Debye length.[48] We hypothesized that in the method presented here, due to the requirement of EOF to generate ion current rectification, the value of R_f could be used to indicate the significance of EOF and the electric double layer for R_f. For example, under conditions when the Debye length was small relative to the diameter of the pore (*e.g.*, $\lambda_D < 0.07$), we measured a R_f value of 6.1 $\pm$ 1.1, a value close to the expected value of 6.2 based on G_f.

The close agreement between the values of R_f and G_f suggests that, under these conditions, the ion current rectification was due to EOF-driven flow of the solution from the anode compartment into the nanopore. This result is in agreement with findings by Taylor and Ren, who demonstrated numerically that the average-area velocity of EOF was only reduced by 5% at $\lambda_D \approx 0.05$ compared to situations where λ_D was less than 0.01.[48] In addition, we did not expect ion current rectification by the classic mechanism in nanopores with this Debye length, because Vlassiouk *et al*. obtained numerically, and Wei *et al*. showed experimentally, values for $R_f \leq 1.5$ when $\lambda_D < 0.07$.[11,21] At these low values of λ_D, electric double layer overlap was not sufficient for the classic mechanism of ion current rectification.

Interestingly, as the Debye length increased ($0.07 < \lambda_D < 0.14$), the value of R_f increased to a maximum of 15 and hence above the value of G_f. An $R_f > G_f$ cannot be explained solely by EOF-driven flow of a solution from the anode compartment into the nanopore. Thus we hypothesized that two complementary effects contributed to R_f in this range of λ_D leading to an increase of R_f beyond G_f: (1) Due to the increasing double layer overlap, EOF began to slow (*i.e.*, the velocity of the flow of the solution from the anode compartment into the nanopore decreased), which permitted mixing of the two solutions in the nanopore. The mixing of the two solutions generated a concentration gradient of DMSO within the pore, which resulted in charge asymmetry within the nanopore due to the different Debye lengths in pure DMSO and in pure water; (2) the Debye length was significant compared to the diameter of the nanopore. Thus, the two requirements for ion current rectification in nanopores by the traditional mechanism might have been met (1, charge asymmetry and 2, an electric double layer similar to the diameter of the pore), which could explain the observed increase in the rectification factor beyond the value of G_f. This hypothesis is supported by results from Taylor and Ren who reported that the average-area velocity of EOF decreased by 19% (to 81%) when the value of λ_D increased from 0.025 to 0.25.[48] Additional support for this hypothesis stems from Vlassiouk *et al*. who demonstrated numerically that the value for R_f increased from a value of ~1.5 at $\lambda_D = 0.07$ to a value of ~4.5 at $\lambda_D = 0.14$.[21,48] Thus, the increased value of R_f is consistent with a decline in the velocity of the EOF, and the presence of an electric double layer large enough to generate ion current rectification in nanopores.

At $\lambda_D > 0.14$, the decline in R_f signified reduced electrostatic asymmetry due to increased electric double layer overlap, and finally at $\lambda_D > 0.96$, the R_f value of 1.1 indicated almost complete electric double layer overlap within the nanopore and confirmed the almost complete loss of EOF. This experimental result is in agreement with theoretical predictions by Rice and Whitehead, who demonstrated numerically that complete electric double layer overlap abolished EOF.[47] Hence, the experiments shown in Figure 5B made it possible to confirm experimentally the beginning of electric double layer overlap at $\lambda_D > 0.14$ and the almost complete removal of EOF at $\lambda_D \geq 0.96$.

EOF-driven Rectification Breaks Down in Very Short Nanopores. To examine ion current rectification in very short pores, in which EOF may be reduced, we used two cylindrical pores with diameters of 30 nm that were fabricated in

silicon nitride membranes. One pore was fabricated in a silicon nitride membrane with a thickness of 275 nm and the other pore in a membrane with a thickness of ~10 nm. When the pore in a 275 nm thick membrane separated solutions containing KCl in 75% (v/v) DMSO and 25% (v/v) water from a solution containing KCl in pure water, we observed values of $R_f = 3.8 \pm 0.3$ using a concentration of 150 mM KCl and $R_f = 4.3 \pm 0.5$ using a concentration of 50 mM KCl. These values of R_f were smaller than $R_f \approx 5$, which we would expect for the electroosmotic diode. In addition, in the pore with a membrane thickness of 10 nm, we observed almost no ion current rectification ($R_f = 1.1-1.4$). To date, no experimental evidence of ion current rectification has been reported in solid-state nanopores with a length of less than 40 nm.[28,32] Together these results suggest that electroosmotic diodes are sensitive to the length of the pore and may only be functional in pore lengths larger than tens of nanometers. In addition, these results provide additional evidence that the ion current rectification that we observed was the result of EOF-driven flow of a low conductance solution from the anode compartment into the nanopore.

CONCLUSION

This paper introduces a simple method for generating fluidic diodes in nano- and microscale pores. This method does not require spatially patterned surface charges, ionic gradients, or pores with a dimension on the order of the Debye screening length to generate ion current rectification. Instead, the ion current rectification is based on electroosmotic flow that moves solutions with different viscosity and hence different conductance into or out of the narrowest constriction of a pore. This approach is different from the electrostatic asymmetry that results in accumulation or depletion of ions within a nanochannel under an applied electric potential. We demonstrate that ion current rectification in this electroosmotic diode is independent of electrolyte concentration in pores with diameters up to ~500 times larger than the Debye length. The extent of ion current rectification could be controlled with different solvent and water mixtures; various rectification factors could be chosen on the basis of the conductance values of the solutions located at the top and at the bottom of the chip. Avoiding EOF within the pore at pH ≈ 0 abolished ion current rectification, and a positive surface charge on the wall of the pore resulted in EOF toward the anode; this reversal of flow resulted in ion current rectification at the opposite polarity of the applied potential difference. In addition, we confirmed that ion current rectification due to EOF was maintained in *nanopores* on the order of the Debye length and that under optimum conditions, the ion current rectification could be amplified due to EOF-driven flow of a solution with a low conductance into the pore in combination with electrostatic asymmetry at the pore openings. The rectification factors of 5−15, that we achieved here, are comparable to methods for generating ion current rectification that rely on ionic strength, pH, or geometry to generate electrostatic asymmetry. This range of R_f values is smaller than R_f values of 100−300 obtained in nanopores with spatially patterned surfaces charges. In addition, similar to other methods for generating ion current rectification, electroosmotic diodes did not rectify current in pores with a length of only 10 nm.

In contrast to existing methods, however, the electroosmotic diodes introduced here make it possible to extend the phenomenon of ion current rectification to pores that are more than 500 times larger than the Debye length, opening the door to microscale fluidic diodes.

We determined the magnitude of ion current rectification as a function of the Debye length, and because the method presented here required electroosmotic flow to generate ion current rectification, we could use the rectification factor to estimate the significance of the electroosmotic flow and of the electric double layer for R_f. Analysis of this data revealed experimentally the values of the nondimensional Debye length at which the electroosmotic flow is significant, reduced, or almost completely abolished. This analysis also revealed the nondimensional Debye length at which (i) the electric double layer can affect ion current rectification, (ii) the electric double layer begins to overlap, and (iii) complete electric double layer overlap occurs. Thus, we demonstrated that R_f as a function of λ_D may be used to confirm experimentally the significance of electroosmotic flow and the electric double layer within nanopores.

METHODS

Solutions and Materials. All aqueous solutions and all water and solvent mixtures contained a final concentration of 15 mM of 4-(2-hydroxyethyl)-1-piperazineethanesulfonic acid (HEPES) buffer and various concentrations of potassium chloride (KCl, which served as the conducting electrolyte). We adjusted the pH of the solutions to 7.4 ± 0.1 by adding hydrochloric acid (HCl) or potassium hydroxide (KOH). We prepared mixtures of KCl solubilized in deionized water ($\rho = 18.2\ M\Omega \cdot cm$, Millipore) and (i) 75% (v/v) dimethyl sulfoxide (DMSO), (ii) 75% (v/v) isopropyl alcohol, or (iii) 66% (v/v) glycerol in such a way that each mixture contained concentrations of KCl (1−200 mM) and HEPES (15 mM) identical to the purely aqueous electrolyte solutions that were used in the opposite compartment of the setup (Figure 1) during the experiments. We filtered all solutions with porous membranes (Pall Acrodisc, Port Washington, NY) that had a pore size of 20 nm. Figure 1 shows the location of the conical pore and of both solutions in the recording device. We measured the conductance of each solution with a calibrated conductivity meter (Orion 5 Star Benchtop Meter, Thermo Electron Corporation, Beverly, MA).

Nano- and Micropores. Following a previously described process, we used a femto-second, pulsed laser followed by an etch

with hydrofluoric acid (HF) to fabricate conical pores with a tip diameter of 500 nm and 2.2 μm in borosilicate glass (thickness ≅ 150 μm, Corning 0211, Fisher Scientific, Pittsburgh, PA).[57−60] Prior to each experiment, we cleaned the glass substrate that contained the conical pores in a freshly prepared, hot mixture of 3:1 (v/v) concentrated sulfuric acid, and 30% hydrogen peroxide for at least 15 min. Where indicated, we incubated the 500 nm pore in an aqueous solution containing 1 mg · mL^{-1} of poly-L-lysine, MW = 15−30 kDa (Sigma Aldrich, St. Louis, MO), for 12 h to generate positive surface charges on the glass substrate.[56] Professor Zuzanna S. Siwy, University of Irvine, CA, kindly provided a cylindrical pore with a diameter of 10 nm fabricated in polyethylene terephthalate (PET) that was 12 μm thick. We used this pore as supplied without cleaning. We also used a cylindrical pore with a diameter of 30 nm that was fabricated by AppNano (Santa Clara, CA) in a silicon nitride membrane with a thickness of 275 nm. Finally, Professor Jiali Li, University of Arkansas, AR, kindly provided a second cylindrical pore with a diameter of 30 nm that was fabricated in a 10 nm thick silicon nitride membrane.[7,8] We cleaned these pores in the same fashion as the pore in glass. To provide support for the substrates that contained the pores and to integrate fluidics, we fabricated a simple poly(dimethylsiloxane) (PDMS, Sylgard 184 Silicone, Dow Corning, Midland, MI) support as shown in Figure 1.

Electrical Recordings. We used Ag/AgCl pellet electrodes (Warner Instruments, Hamden, CT) to record ion currents. For each recording, we placed the experimental setup in a Faraday cage (Warner Instruments, Hamden, CT). We recorded the electrical current using a patch-clamp amplifier (Axopatch 200B, Molecular Devices Inc.) in voltage clamp mode with the analog low-pass filter set to a cutoff frequency of 2 kHz. In voltage clamp mode, the amplifier can apply a maximum voltage of ±1 V while measuring currents in the range of <0.1 pA up to 200 nA. We set the gain of the amplifier to 1 mV · pA^{-1} (*i.e.*, β = 1) to measure currents below 20 nA and to 0.1 mV · pA^{-1} (*i.e.*, β = 0.1) to measure currents below 200 nA. We used a low noise digitizer (Digidata 1322) with a sampling frequency set to 5 times the low pass cutoff frequency in combination with LabView recording software for all recordings. We performed all data processing using Clampfit 9.2 (Axon Instruments, Union City, CA). At each applied potential, we averaged the current over a period of 10 s, hence averaging 100,000 current values, to obtain current−voltage plots. To measure currents above 200 nA we used a picoammeter (Keithley Instruments, Inc., Cleveland, OH). We calculated the average current value and standard deviation from three independent observations.

Acknowledgment. This work was supported by a National Science Foundation Career Award (M.M., Grant No. 0449088). The authors thank Daniel J. Estes, Ph.D. and Jeffrey D. Uram, Ph.D. for their work on the LabView recording software.

REFERENCES AND NOTES

1. Han, J. H.; Kim, K. B.; Kim, H. C.; Chung, T. D. Ionic Circuits Based on Polyelectrolyte Diodes on a Microchip. *Angew. Chem., Int. Ed.* **2009**, *48*, 3830–3833.
2. Ali, M.; Mafe, S.; Ramirez, P.; Neumann, R.; Ensinger, W. Logic Gates Using Nanofluidic Diodes Based on Conical Nanopores Functionalized with Polyprotic Acid Chains. *Langmuir* **2009**, *25*, 11993–11997.
3. Chang, H.; Venkatesan, B. M.; Iqbal, S. M.; Andreadakis, G.; Kosari, F.; Vasmatzis, G.; Peroulis, D.; Bashir, R. DNA Counter-ion Current and Saturation Examined by a Mems-Based Solid State Nanopore Sensor. *Biomed. Microdevices* **2006**, *8*, 263–269.
4. Kalman, E. B.; Vlassiouk, I.; Siwy, Z. S. Nanofluidic Bipolar Transistors. *Adv. Mater.* **2008**, *20*, 293–297.
5. Smeets, R. M. M.; Keyser, U. F.; Krapf, D.; Wu, M. Y.; Dekker, N. H.; Dekker, C. Salt Dependence of Ion Transport and DNA Translocation through Solid-State Nanopores. *Nano Lett.* **2006**, *6*, 89–95.
6. Storm, A. J.; Chen, J. H.; Ling, X. S.; Zandbergen, H. W.; Dekker, C. Fabrication of Solid-State Nanopores with Single-Nanometre Precision. *Nat. Mater.* **2003**, *2*, 537–540.
7. Li, J.; Stein, D.; McMullan, C.; Branton, D.; Aziz, M. J.; Golovchenko, J. A. Ion-Beam Sculpting at Nanometre Length Scales. *Nature* **2001**, *412*, 166–169.
8. Cai, Q.; Ledden, B.; Krueger, E.; Golovchenko, J. A.; Li, J. L. Nanopore Sculpting with Noble Gas Ions. *J. Appl. Phys.* **2006**, *100*, 024914.
9. Davenport, M.; Rodriguez, A.; Shea, K. J.; Siwy, Z. S. Squeezing Ionic Liquids through Nanopores. *Nano Lett.* **2009**, 2125–2128.
10. Siwy, Z.; Heins, E.; Harrell, C. C.; Kohli, P.; Martin, C. R. Conical-Nanotube Ion-Current Rectifiers: The Role of Surface Charge. *J. Am. Chem. Soc.* **2004**, *126*, 10850–10851.
11. Wei, C.; Bard, A. J.; Feldberg, S. W. Current Rectification at Quartz Nanopipet Electrodes. *Anal. Chem.* **1997**, *69*, 4627–4633.
12. Vlassiouk, I.; Siwy, Z. S. Nanofluidic Diode. *Nano Lett.* **2007**, *7*, 552–556.
13. Siwy, Z.; Fulinski, A. Fabrication of a Synthetic Nanopore Ion Pump. *Phys. Rev. Lett.* **2002**, *89*, 198103.
14. Apel, P. Y.; Korchev, Y. E.; Siwy, Z.; Spohr, R.; Yoshida, M. Diode-like Single-Ion Track Membrane Prepared by Electro-Stopping. *Nucl. Instrum. Methods Phys. Res., Sect. B* **2001**, *184*, 337–346.
15. Hille, B. *Ion Channels of Excitable Membranes;* Sinauer Associaties, Inc.: Sunderland, MA, 2001.
16. Gatimu, E. N.; King, T. L.; Sweedler, J. V.; Bohn, P. W. Three-Dimensional Integrated Microfluidic Architectures Enabled through Electrically Switchable Nanocapillary Array Membranes. *Biomicrofluidics* **2007**, *1*, 021502.
17. Miller, S. A.; Kelly, K. C.; Timperman, A. T. Ionic Current Rectification at a Nanofluidic/Microfluidic Interface with an Asymmetric Microfluidic System. *Lab Chip* **2008**, *8*, 1729–1732.
18. Kalman, E. B.; Sudre, O.; Vlassiouk, I.; Siwy, Z. S. Control of Ionic Transport through Gated Single Conical Nanopores. *Anal. Bioanal. Chem.* **2009**, *394*, 413–419.
19. Ali, M.; Mafe, S.; Ramirez, P.; Neumann, R.; Ensinger, W. Logic Gates Using Nanofluidic Diodes Based on Conical Nanopores Functionalized with Polyprotic Acid Chains. *Langmuir* **2009**, *25*, 11993–11997.
20. Siwy, Z.; Trofin, L.; Kohli, P.; Baker, L. A.; Trautmann, C.; Martin, C. R. Protein Biosensors Based on Biofunctionalized Conical Gold Nanotubes. *J. Am. Chem. Soc.* **2005**, *127*, 5000–5001.
21. Vlassiouk, I.; Kozel, T. R.; Siwy, Z. S. Biosensing with Nanofluidic Diodes. *J. Am. Chem. Soc.* **2009**, *131*, 8211–8220.
22. Siwy, Z. S. Ion-Current Rectification in Nanopores and Nanotubes with Broken Symmetry. *Adv. Funct. Mater.* **2006**, *16*, 735–746.
23. Cheng, L. J.; Guo, L. J. Ionic Current Rectification, Breakdown, and Switching in Heterogeneous Oxide Nanofluidic Devices. *ACS Nano* **2009**, *3*, 575–584.
24. Israelachvili, J. *Intermolecular and Surface Forces,* 2nd Ed.; Academic Press: London, 2003.
25. Mayer, M. Screeening for Bioactive Compounds: Chip-Based Functional Analysis of Single Ion Channels & Capillary Electrochromatography for Immunoaffinity Selection. In *Department of Biotechnology;* Swiss Federal Institute of Technology: Lausanne, Switzerland. 2000; p 131.
26. Constantin, D.; Siwy, Z. S. Poisson−Nernst−Planck Model of Ion Current Rectification through a Nanofluidic Diode. *Phys. Rev. E* **2007**, *76*, 041202.
27. Aidan, P. T. Nonequilibrium Molecular Dynamics Simulation of Electro-Osmotic Flow in a Charged Nanopore. *J. Chem. Phys.* **2003**, *119*, 7503–7511.
28. Vlassiouk, I.; Smirnov, S.; Siwy, Z. Nanofluidic Ionic Diodes. Comparison of Analytical and Numerical Solutions. *ACS Nano* **2008**, *2*, 1589–1602.
29. Siwy, Z.; Gu, Y.; Spohr, H. A.; Baur, D.; Wolf-Reber, A.; Spohr, R.; Apel, P.; Korchev, Y. E. Rectification and Voltage Gating of Ion Currents in a Nanofabricated Pore. *Europhys. Lett.* **2002**, *60*, 349–355.

30. Siwy, Z.; Apel, P.; Baur, D.; Dobrev, D. D.; Korchev, Y. E.; Neumann, R.; Spohr, R.; Trautmann, C.; Voss, K.-O. Preparation of Synthetic Nanopores with Transport Properties Analogous to Biological Channels. *Surf. Sci.* **2003**, *532*−*535*, 1061–1066.
31. White, H. S.; Bund, A. Ion Current Rectification at Nanopores in Glass Membranes. *Langmuir* **2008**, *24*, 2212–2218.
32. Chen, P.; Mitsui, T.; Farmer, D. B.; Golovchenko, J.; Gordon, R. G.; Branton, D. Atomic Layer Deposition to Fine-Tune the Surface Properties and Diameters of Fabricated Nanopores. *Nano Lett.* **2004**, *4*, 1333–1337.
33. Cervera, J.; Schiedt, B.; Ram, P. A Poisson/Nernst−Planck Model for Ionic Transport through Synthetic Conical Nanopores. Europhys. *Lett.* **2005**, *71*, 35–41.
34. Ali, M.; Ramirez, P.; Mafe, S.; Neumann, R.; Ensinger, W. A Ph-Tunable Nanofluidic Diode with a Broad Range of Rectifying Properties. *ACS Nano* **2009**, *3*, 603–608.
35. Ali, M.; Schiedt, B.; Healy, K.; Neumann, R.; Ensinger, A. Modifying the Surface Charge of Single Track-Etched Conical Nanopores in Polyimide. *Nanotechnology* **2008**, *19*, 085713.
36. Cheng, L.-J.; Guo, L. J. Rectified Ion Transport through Concentration Gradient in Homogeneous Silica Nanochannels. *Nano Lett.* **2004**, *7*, 3165–3171.
37. Fulinski, A.; Kosinska, I. D.; Siwy, Z. On the Validity of Continuous Modelling of Ion Transport through Nanochannels. *Europhys. Lett.* **2004**, *67*, 683–689.
38. Scruggs, N. R.; Robertson, J. W. F.; Kasianowicz, J. J.; Migler, K. B. Rectification of the Ionic Current through Carbon Nanotubes by Electrostatic Assembly of Polyelectrolytes. *Nano Lett.* **2009**, *9*, 3853–3859.
39. Hammann, C. H.; Hamnett, A.; Vielstich, W. *Electrochemistry*. Wiley-VCH: New York, 1998.
40. Cervera, J.; Alcaraz, A.; Schiedt, B.; Neumann, R.; Ramirez, P. Asymmetric Selectivity of Synthetic Conical Nanopores Probed by Reversal Potential Measurements. *J. Phys. Chem. C* **2007**, *111*, 12265–12273.
41. Cheng, L.-J. Ion and Molecule Transport in Nanochannels. In *Electrical Engineering and Computer Science;* University of Michigan: Ann Arbor, MI., 2008; p 141.
42. Ali, M.; Yameen, B.; Neumann, R.; Ensinger, W.; Knoll, W.; Azzaroni, O. Biosensing and Supramolecular Bioconjugation in Single Conical Polymer Nanochannels. Facile Incorporation of Biorecognition Elements into Nanoconfined Geometries. *J. Am. Chem. Soc.* **2008**, *130*, 16351–16357.
43. Yameen, B.; Ali, M.; Neumann, R.; Ensinger, W.; Knoll, W.; Azzaroni, O. Single Conical Nanopores Displaying Ph-Tunable Rectifying Characteristics. Manipulating Ionic Transport with Zwitterionic Polymer Brushes. *J. Am. Chem. Soc.* **2009**, *131*, 2070–2071.
44. Sandip, G. Fluid Mechanics of Electroosmotic Flow and Its Effect on Band Broadening in Capillary Electrophoresis. *Electrophoresis* **2004**, *25*, 214–228.
45. Pennathur, S.; Santiago, J. G. Electrokinetic Transport in Nanochannels. 1. Theory. *Anal. Chem.* **2005**, *77*, 6772–6781.
46. Pennathur, S.; Santiago, J. G. Electrokinetic Transport in Nanochannels. 2. Experiments. *Anal. Chem.* **2005**, *77*, 6782–6789.
47. Rice, C. L.; Whitehead, R. Electrokinetic Flow in a Narrow Cylindrical Capillary. *J. Phys. Chem-US.* **1965**, *69*, 4017–4024.
48. Taylor, J.; Ren, C. L. Application of Continuum Mechanics to Fluid Flow in Nanochannels. *Microfluid. Nanofluid.* **2005**, *1*, 356–363.
49. Kemery, P. J.; Steehler, J. K.; Bohn, P. W. Electric Field Mediated Transport in Nanometer Diameter Channels. *Langmuir* **1998**, *14*, 2884–2889.
50. Daiguji, H.; Yang, P.; Majumdar, A. Ion Transport in Nanofluidic Channels. *Nano Lett.* **2004**, *4*, 137–142.
51. Vlassiouk, I.; Smirnov, S.; Siwy, Z. Ionic Selectivity of Single Nanochannels. *Nano Lett* **2008**, *8*, 1978–1985.
52. Shun-Cheng, W.; Tzu-Chien, W.; Wun-Bin, C.; Heng-Kwong, T. Effects of Surfactant Micelles on Viscosity and Conductivity of Poly(ethylene glycol) Solutions. *J. Chem. Phys.* **2004**, *120*, 4980–4988.
53. Barthel, J.; Bachhuber, K.; Buchner, R.; Hetzenauer, H. Dielectric Spectra of Some Common Solvents in the Microwave Region. Water and Lower Alcohols. *Chem. Phys. Lett.* **1990**, *165*, 369–373.
54. Barthel, J.; Bachhuber, K.; Buchner, R.; Gill, J. B.; Kleebauer, M. Dielectric Spectra of Some Common Solvents in the Microwave Region. Dipolar Aprotic Solvents and Amides. *Chem. Phys. Lett.* **1990**, *167*, 62–66.
55. Ermakova, L. E.; Sidorova, M.; Jura, N.; Savina, I. Adsorption and Electrokinetic Characteristics of Micro- and Macroporous Glasses in 1:1 Electrolytes. *J. Membr. Sci.* **1997**, *131*, 125–141.
56. Schmidt, C.; Mayer, M.; Vogel, H. A Chip-Based Biosensor for the Functional Analysis of Single Ion Channels. *Angew. Chem. Int. Ed.* **2000**, *39*, 3137–3140.
57. Uram, J. D.; Ke, K.; Mayer, M. Noise and Bandwidth of Current Recordings from Submicrometer Pores and Nanopores. *ACS Nano* **2008**, *2*, 857–872.
58. An, R.; Uram, J. D.; Yusko, E. C.; Ke, K.; Mayer, M.; Hunt, A. J. Ultrafast Laser Fabrication of Submicrometer Pores in Borosilicate Glass. *Opt. Lett.* **2008**, *33*, 1153–1155.
59. Uram, J. D.; Ke, K.; Hunt, A. J.; Mayer, M. Label-Free Affinity Assays by Rapid Detection of Immune Complexes in Submicrometer Pores. *Angew. Chem., Int. Ed.* **2006**, *45*, 2281–2285.
60. Uram, J. D.; Ke, K.; Hunt, A. J.; Mayer, M. Submicrometer Pore-Based Characterization and Quantification of Antibody−Virus Interactions. *Small* **2006**, *2*, 967–972.